The improvements of LLRF control system for CSNS LINAC

Linyan Rong, Yuan Yao, Xinan Xu, Wenzhong Zhou, Meifei Liu, Bo Wang, Zhencheng Mu, Zonghua Zhang, Jimin Qiao, Jian Li
Institute of High Energy Physics, Beijing, China

Abstract

In the finished ADS (Accelerator Driven Sub-critical system) project which supported by China 973 Program in the Institute of High Energy Physics, Chinese Academy of Sciences (IHEP, CAS), a 352.2MHz klystron RF power source was used to drive 3.5MeV RFQ accelerator. On this test stand, we carried out R&D of digital low level RF (LLRF) control system prototype for CSNS LINAC RF system. Based on step-by-step successful R&D and operation experience, many important progresses have been achieved. In design of the process, all analog modules were thermostatically controlled by a temperature stabilizing crate, the related circuits of both cavity field signal and reference signal were designed symmetrically. In design of the control software, the FPGA-based feedback control algorithm has been optimized, and some useful functions were added, such as 1) measuring of cavity Q value, detuning phase and frequency shift, 2) automatic frequency matching for cavity warm-up, 3) using feedforward to compensate the amplitude and phase decrease caused by klystron high voltage droop, 4) RF power monitoring and real-time VSWR protection. The improvements and test results of the LLRF control system for CSNS LINAC will be described in this paper.

INTRODUCTION

We carried out R&D of digital low level RF (LLRF) control system prototype for CSNS LINAC RF system on the 352.2MHz klystron RF power source which was used to drive 3.5MeV RFQ accelerator. On October 2007, LLRF prototype passed acceptance test under RFQ beam commissioning [1], then it had been successfully applied in the operation of the 3.5MeV RFQ accelerator until December 2012. During the several years, many important progresses have been achieved in the LLRF control system for a more-convenient operation and a higher stability performance. On June 2012, the test results show that the amplitude and phase variations in the RFQ cavity are less than ±0.3% and ±0.3° without beam loading, or ±0.4% and ±0.6° with beam loading, much better than the requirements of ± 1% in amplitude and ± 1° in phase [2]. The block diagram and picture of LLRF prototype are shown in Figure 1. Based on the success of LLRF prototype, the LLRF control system which will be applied in the operation of CSNS 324MHz LINAC is being developed.

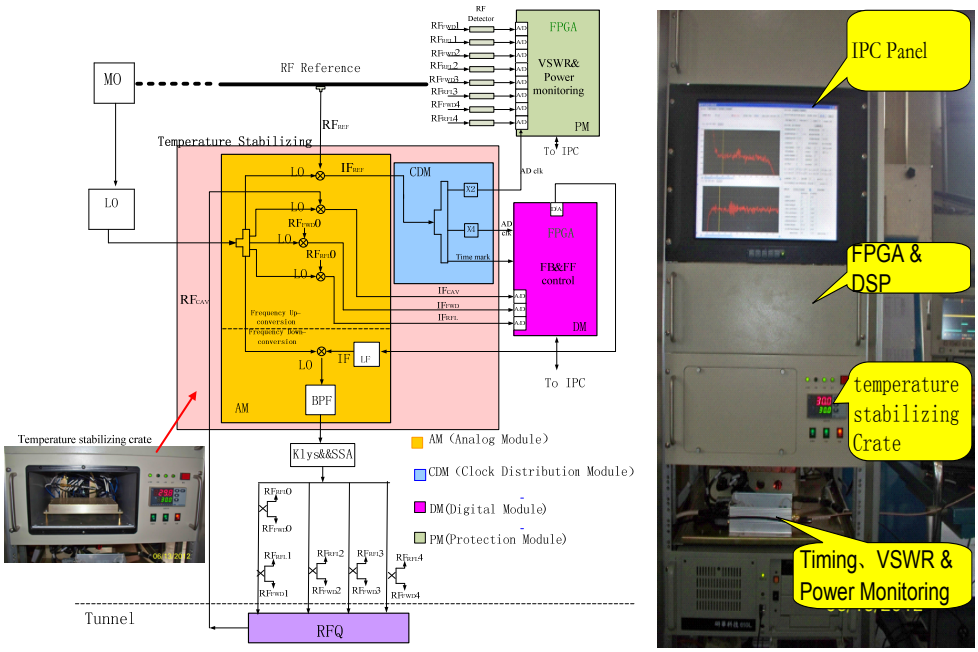

Figure 1：Block diagram and picture of LLRF prototype

PROCESS

Temperature Control of Analog Hardware

The filters, mixers and amplifiers associated with the analog front end board and the RF Output board’s frequency conversion circuits were found to be the cause of small temperature related drifts in RF phase [3]. To avoid these instability, all analog hardware are placed into a temperature stabilizing crate, including frequency down-conversion, up-conversion module and clock distribution module, and the control temperature is maintained at 30 +/- 0.1 degrees Celsius. Semiconductor thermostat is applied in the temperature stabilizing crate, and the regulation is provided by automatic PID bilateral control system with insulation surrounding analog module and RF cables. The picture of temperature stabilizing crate is shown in Figure 1.

Design Strategy of RF Reference

Thermostatically controlled RF reference line of CSNS LINAC will be installed in auxiliary tunnel closed to accelerator cavity in tunnel. 324MHz RF is chosen as the frequency of reference which is the same as the cavity RF, in order to conveniently compare the phase of the two. That should also greatly simplify the installation and initial commissioning [4]. As shown in Figure 2, cavity field signal and reference RF signal are sent from auxiliary tunnel to LLRF controller through a matched cable pair along the same-length path. In addition, the down converted related circuits of both cavity field signal and reference signal are designed symmetrically. Due to this balanced circuit topology, any temperature fluctuation will equally affect the phase of both the cavity field signal cable and the reference cable, and the phase of the cavity IF is measured against the reference IF [4]. So the phase error of both the cavity field signal cable and the reference cable which is caused by temperature fluctuation will be eliminated, the cavity phase to be measured could reflect back the information of cavity.

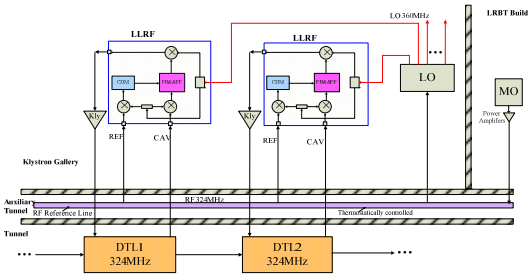

Figure 2: Block diagram of CSNS LLRF reference system

SOFTWARE

Based on step-by-step successful R&D and operation experience, the FPGA-based feedback control algorithm has been optimized, and some useful functions were added, that will be described in the following sections. The block diagram of algorithm in the FPGA is shown in Figure 3.

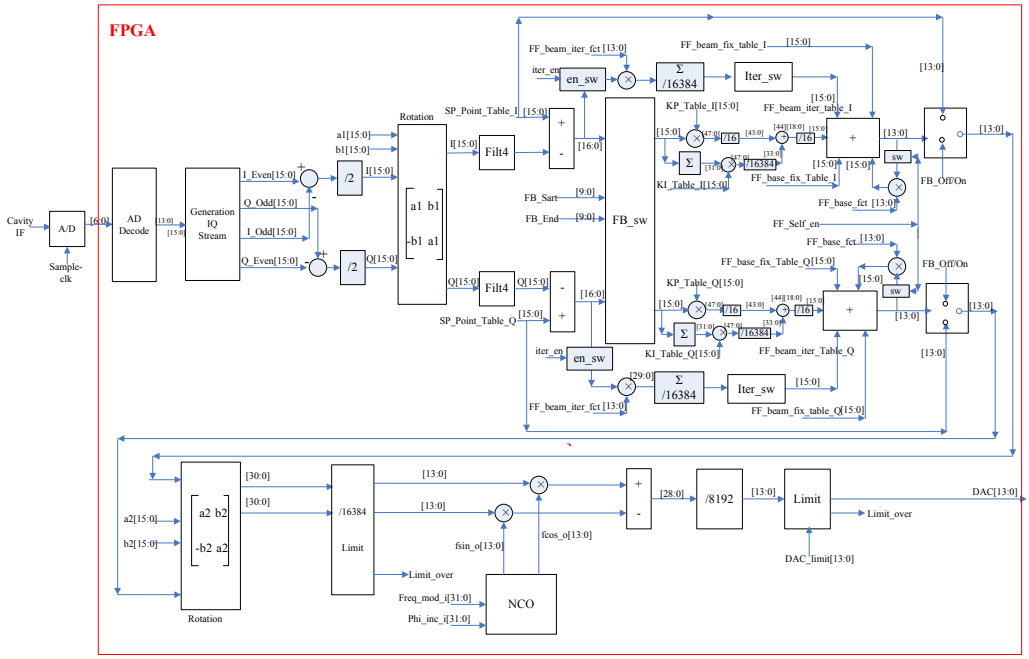

Figure 3: Block diagram of algorithm in the FPGA

Measuring Cavity Q Value, Detuning Phase and Frequency

Two methods are adopted to judge whether the RF cavity is close to the resonance state or not in CSNS LLRF control system. The first method is to detect the phase difference between the cavity input and output signals and to see whether it's the same as that for resonance state. The second method is to detect the phase curve of the RF cavity during the field decay and to see whether the phase is a constant. And, from the field decay curve of amplitude and phase, as shown in Figure 4, cavity characteristics parameters can be calculated out in every pulse, such as time constant of decay, Q value, detuning frequency Δf and detuning phase Δφ. These above parameters are calculated in the DSP.

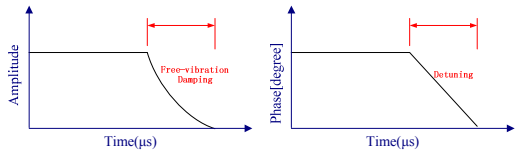

Figure 4: The field decay curve of amplitude and phase

As shown in Figure 4, during free-vibration damping, the amplitude curve of RF cavity can be expressed as equation (1).

$$AMP = Ke^{-\alpha t} = Ke^{-t/\tau} \qquad (1)$$

where τ is the time constant of decay.

By making a logarithm transform for equation (1), we can obtain linear equation (2).

$$Ln(AMP) = LnK - t/\tau \qquad (2)$$

So, the time constant of decay can be calculated out by least square linear fitting at some sampling points.

In order to obtain a more accurate calculation, we take a certain number points of amplitude coordinate for least square fitting, during the free-vibration damping, fitted points are $(t_0, Ln(AMP_0))$, $(t_1, Ln(AMP_1))\ldots(t_{n-1}, Ln(AMP_{n-1}))$. Just after least square fitting, the time constant of decay can be calculated out by equation (3),

$$\tau = -\frac{n\sum_{i=0}^{n-1} t_i^2 - \sum_{i=0}^{n-1} t_i \bullet \sum_{i=0}^{n-1} t_i}{n\sum_{i=0}^{n-1} Ln(AMP_i)\bullet t_i - \sum_{i=0}^{n-1} t_i \bullet \sum_{i=0}^{n-1} Ln(AMP_i)} \qquad (3)$$

Then, the loaded Q-value of cavity is carried out:

$$Q = \frac{\omega_{rf}}{2} \times \tau \qquad (4)$$

where ω_{rf} is the resonance angular frequency of cavity.

As shown in Figure 4, during free-vibration damping, the relationship between phase of RF cavity and time can be expressed as equation (5).

$$\theta = b + \Delta\omega \bullet t \qquad (5)$$

Through least square linear fitting, detuning angular frequency can be calculated out by equation (6).

$$\Delta\omega = \frac{n\sum_{i=0}^{n-1}(\theta_i \bullet t_i) - \sum_{i=0}^{n-1} t_i \bullet \sum_{i=0}^{n-1} \theta_i}{n\sum_{i=0}^{n-1} t_i^2 - \sum_{i=0}^{n-1} t_i \bullet \sum_{i=0}^{n-1} t_i} \qquad (6)$$

where the points used to calculate are(t_0 , θ_0), $(t_1, \theta_1)\ldots(t_{n-1}, \theta_{n-1})$.

Then, the detuning frequency and phase of cavity are calculated out:

$$\Delta f = \frac{1}{2\pi} \times \Delta\omega \quad (7), \qquad \Delta\varphi = \tan^{-1}\left(2Q\frac{\Delta f}{f_{rf}}\right) \quad (8)$$

where f_{rf} is resonance frequency.

At the end of RF pulse, the phase curve of RF cavity will be close to flat, when Δf is close to zero. Figure 5 shows an example which was measured at the commissioning of 3.5MeV RFQ accelerator. As shown in Figure 5(b) and (c), blue dot line is measured value, red line is fitting curve by least square method. The two lines nearly coincide. The time constant of decay is 2.56μs, the loaded Q-value of cavity is 2810, detuning frequency and phase of cavity are 17.06kHz, 15.23°, respectively [2].

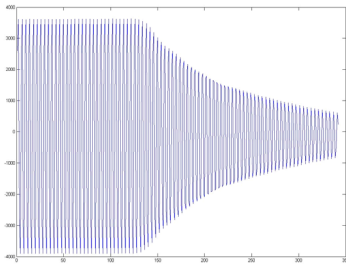

(a): original ADC sample data

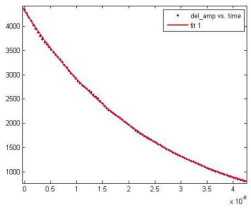

(b): Field amplitude

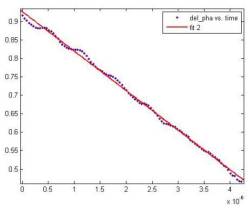

(c): Field phase

Figure 5: An example

Automatic Frequency Matching for Cavity Warm-up

The RF power is reflected by detuned cavity, when cold cavity starts up. The new method of automatic frequency matching for cavity warm-up is applied in CSNS LLRF control system. Block diagram of automatic frequency matching for cavity warm-up is shown in Figure 6. Based on above Δf calculation in every pulse, via phase scan algorithm in FPGA, cavity input

frequency can be change to automatically match with cold cavity natural frequency.

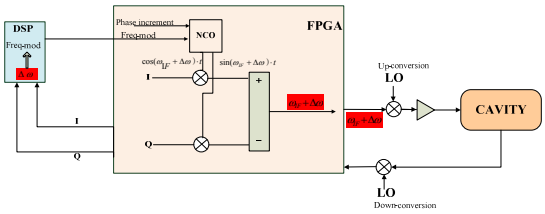

Figure 6: Block diagram of automatic frequency matching for cavity warm-up

When LLRF control system operates in the mode of FB on, as shown in Figure 6, the value of Freq-mod is set to zero, and then $\cos\omega_{IF}\cdot t$ and $\sin\omega_{IF}\cdot t$ are outputted by NCO. In the mode of automatic frequency matching, the Freq-mod can be calculated out by equation (9). And $\cos(\omega_{IF}+\Delta\omega)\cdot t$、$\sin(\omega_{IF}+\Delta\omega)\cdot t$ are outputted by NCO.

$$Freq-\mathrm{mod}=\frac{\Delta f\cdot 2^{32}}{f_{clk}} \qquad (9)$$

In CSNS LLRF control system, clock rate f_{clk} is 144MHz, intermediate Frequency (IF) is 36 MHz, so the value of IF phase increments is 1044721775.

By using this method, the RF power could be fed into the detuned cavity successfully without significant reflection, then the time of cavity warm-up is greatly shorten. Figure 7 shows an example of the waveforms of RF cavity during the RF start-up at the 3.5MeV RFQ accelerator.

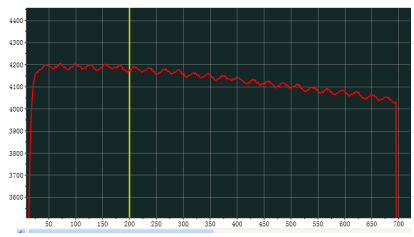

(a)Amplitude

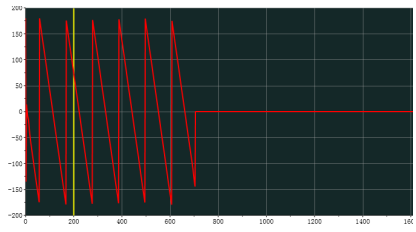

(b)Phase

Figure 7: Waveforms of RF cavity during the RF start-up

Feedforward Compensation

The amplitude and phase of cavity decreased, due to the klystron high voltage droop. This droop is repetitive errors from pulse to pulse in a period of time. So, improved feedforward is adopted to deal with the repetitive errors.

At first, we can obtain the drooped waveform of cavity caused by the klystron high voltage droop, as shown in Figure 8, under condition of FB off and RF cavity closed to resonance state.

Then, FB on, I, Q values processed by PI control in the FPGA are read back to feedforward table, which is called as FF_base_table, and FF_base_table waveform is showed in Figure 9. So, the drooped amplitude of cavity caused by the klystron high voltage droop is compensated, when FF_base_table is added in FB control.

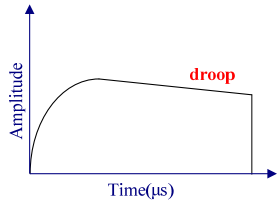

Figure 8: FB off, the waveform of cavity

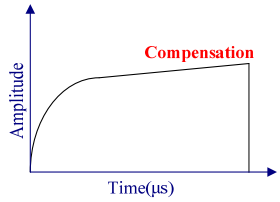

Figure 9: Waveform of FF_base_table

RF Power Monitoring and Real-time VSWR Protection

RF power detection and VSWR protection is implemented by Power Protection Module (PM), Block diagram of PM is shown in Figure 10. The PM module can monitor up to eight RF channels. RF signals are detected by logarithmic detector, and then are sampled by 14bit-ADCs. The fault detection logic is implemented in a single FPGA. Industry PC provides monitoring for eight channels RF power and four channels VSWR.

There are two modes for RF block. The first mode is auto-recovered RF block, if detecting VSWR is over defined threshold, the RF drive and beam shall be inhibited within 1μs of the detection and shall be re-enabled in the following pulse. The second mode is permanent RF block, if detecting VSWR protection take place N times in a second, The RF drive and beam shall be permanently blocked.

The response time from detecting VSWR over-limit until the RF drive is inhibited less

than 460nS, as shown in Figure 11.

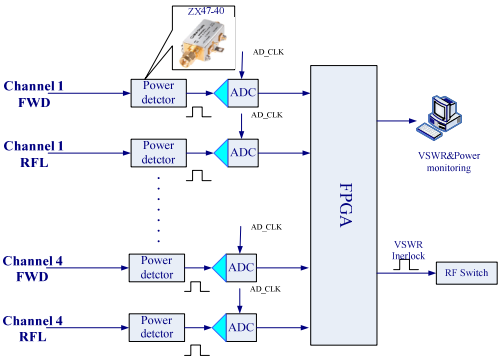

Figure10: Block diagram of PM

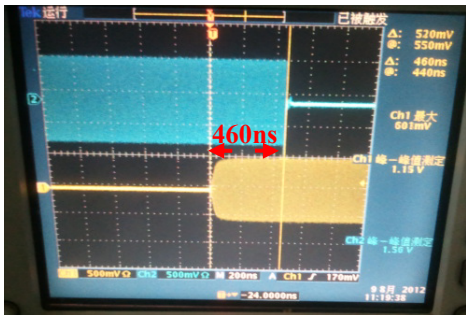

Figure 11: Response of VSWR over-limit

ACKNOWLEDGEMENTS

The authors would like to thank the No. 23 Institute of China Aerospace Science and Industry for the construction of the digital LLRF control system. Thanks are also due to Z. Fang (KEK) for many useful discussions.

REFERENCES

[1] Jian Li, et al., "CSNS LINAC RF System Design and R&D Progress", Proc. of the LINAC2010, THP046, 2010.

[2] Jian Li, et al., "R&D Progress of CSNS LINAC RF System ", Proc. of 6th China RF and microwave, 2012.

[3] Mark Crofford, et al., "Spallation Neutron Source LLRF Temperature Dependence and Solution", Proc. of the LINAC2010, MOP088, 2010.

[4] Hengjie Ma, "SNS LINAC RF Control: Reference System and Phase Measurement", SNS LLRF Tech Note 3, 2002.